

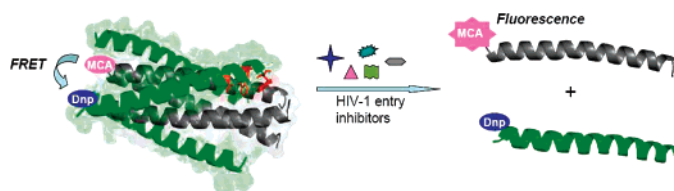
Development of a FRET Assay for Monitoring of HIV gp41 Core Disruption

Yang Xu,[†] Mark S. Hixon,[‡] Philip E. Dawson,[§] and Kim D. Janda^{*,†}

Department of Chemistry and Immunology and The Skaggs Institute for Chemical Biology and Worm Institute for Research and Medicine (WIRM), The Scripps Research Institute, 10550 North Torrey Pines Road, La Jolla, California 92037

kdjanda@scripps.edu

Received April 24, 2007



The fusogenic core assembly of human immunodeficiency virus type 1 (HIV-1) fusion protein gp41 is a critical transformation for viral entry. Molecules that are able to intercept this process are of great therapeutic value as HIV-1 fusion inhibitors. In the search for such molecules, assay systems that can be adapted to high-throughput screens are valuable. Given that gp41 fusogenic transformation is characterized by the hexameric association of heptads located at the N and C terminal regions of the protein ectodomain, the corresponding heptad peptides (CHR and NHR), known to form the six-helix bundle core of gp41 fusion active form, are potentially useful in developing a fluorescence resonance energy transfer (FRET) system for identification of HIV fusion inhibitors. We demonstrate that by strategically placing two FRET probes on these two peptides, we are able to monitor the intermolecular co-association by fluorescence quenching between the fluorescence donor and acceptor. The utility of the system is that it should be adaptable to high-throughput screening (HTS) toward peptide or small-molecule HIV fusion inhibitors targeting the gp41 core. Herein, we report the design, synthesis, and development of a N- and C-terminal peptide FRET pair for screening of gp41 six-helix bundle disruption.

Introduction

Human immunodeficiency virus type 1 (HIV-1) enters target cells by fusion of the viral envelope and target cell membrane, followed by release of viral genetic material into the cell.^{1,2} One of the key players mediating this process is gp41, a viral envelope (Env) glycoprotein derived from the precursor protein gp160 by proteolytic processing.^{3–5} Therefore, gp41 serves as

a promising target for the development of therapeutics targeting the viral fusion process.^{6,7}

Protein dissection studies and X-ray crystallographic data have revealed that the NHR and CHR regions of gp41, modeled by N- and C-terminal peptides, co-associate to form a helical trimer of antiparallel dimers in the fusion-active gp41 core domain.^{8–10} The inner coiled-coil trimer is formed by the leucine zipper-like heptad repeat sequence, while the outer trimer of C-helices

[†] Department of Chemistry and Immunology and The Skaggs Institute for Chemical Biology and Worm Institute for Research and Medicine.

[‡] Current address: Takeda San Diego Inc. 10410 Science Center Drive San Diego, California 92121.

[§] Department of Cell Biology and Chemistry and The Skaggs Institute for Chemical Biology, The Scripps Research Institute, 10550 North Torrey Pines Road, La Jolla, California 92037.

(1) Chen, Y. H.; Xiao, Y.; Dierich, M. P. *Prog. Nat. Sci.* **2000**, *10*, 91–95.

(2) Clapham, P. R.; McKnight, A.; Talbot, S.; Wilkinson, D. *Perspect. Drug Discovery* **1996**, *5*, 83–92.

(3) Gallo, S. A.; Finnegan, C. M.; Viard, M.; Raviv, Y.; Dimitrov, A.; Rawat, S. S.; Puri, A.; Durell, S.; Blumenthal, R. *BBA-Biomembr.* **2003**, *1614*, 36–50.

(4) Ferris, R. L.; Hall, C.; Sipsas, N. V.; Safrit, J. T.; Trocha, A.; Koup, R. A.; Johnson, R. P.; Siliciano, R. F. *J. Immunol.* **1999**, *162*, 1324–1332.

(5) Callahan, K. M.; Rowell, J. F.; Soloski, M. J.; Machamer, C. E.; Siliciano, R. F. *J. Immunol.* **1993**, *151*, 2928–2942.

(6) Jiang, S. B.; Zhao, Q.; Debnath, A. K. *Curr. Pharm. Des.* **2002**, *8*, 563–580.

(7) Turpin, J. A.; Howard, O. M. Z. *Expert Opin. Ther. Pat.* **2000**, *10*, 1899–1909.

(8) Golding, H.; Zaitseva, M.; de Rosny, E.; King, L. R.; Manischewitz, J.; Sidorov, I.; Gorny, M. K.; Zolla-Pazner, S.; Dimitrov, D. S.; Weiss, C. D. *J. Virol.* **2002**, *76*, 6780–6790.

(9) Lu, M.; Kim, P. S. *J. Biomol. Struct. Dyn.* **1997**, *15*, 465–471.

(10) Lu, M.; Ji, H.; Shen, S. *J. Virol.* **1999**, *73*, 4433–4438.

packs in an antiparallel fashion into the grooves on the surface of the inner trimer. The C-helix interacts with the N-helix through hydrophobic amino acid residues located in the N-helix grooves; these amino acid residues are highly conserved in most HIV strains.

Compounds that are able to disrupt the formation of the six-helix bundle core have promising potential as HIV-1 fusion inhibitors. Previously it has been reported that both N- and C-terminal peptides have inhibitory activities against the fusion of HIV or HIV-infected cells with uninfected cells, with C-peptides being more potent than N-peptides.^{11–13} In efforts to uncover such HIV-1 fusion inhibitors, a number of systems have been developed, including several ELISA assays that utilize a six-helix bundle recognizing mAb, NC1.^{14–16}

On the basis of C- and N-helix interactions found in the gp41 core domain, we propose that the placement of two fluorescence resonance energy transfer (FRET) probes on these two peptides will allow the monitoring of the intermolecular co-association as reported by fluorescence quenching between the fluorescence donor and acceptor. Furthermore, such a system could be applied to high-throughput screening (HTS) toward peptide or small-molecule HIV-1 fusion inhibitors targeting gp41 core. Herein, we report the design, synthesis, and development of a novel N- and C-terminal peptide FRET pair for the screening of gp41 six-helix bundle disruption.

Results and Discussion

1. Synthesis of a N- and C-Terminal Peptide FRET Pair for Screening of gp41 Six-Helix Bundle Disruption. We have chosen a well-known FRET pair, 7-methoxycoumarin-4-acetic acid (MCA) and 2,4-dinitrophenyl (Dnp) groups as fluorophore and quencher, respectively (Figure 1A). This FRET pair is attractive by virtue of the small size of these chemical moieties; the avoidance of large polycyclic FRET pairs (e.g., fluorescein isothiocyanate/4-(dimethylaminoazo)benzene-4-carboxylic acid (FITC/Dabcyl)) is desirable to minimize perturbation of N36/C34 complexation. Additionally, the use of larger FRET pairs is contraindicated—despite their lower detection limits stemming from increased quantum yields—because they could plausibly interact with peptide or nonpeptide inhibitors via π -stacking interactions and confound results.

We recognize that in developing this FRET peptide pair, it is critical to place the donor and quencher probes at sites such to minimize any disturbance to the six-helix bundle assembly. It is also important to note that the prominent pocket for the binding of fusion inhibitors reported previously by Chan et al. should not be occluded or otherwise affected by addition of the FRET probes.^{17,18} Chan has reported that each C helix shows

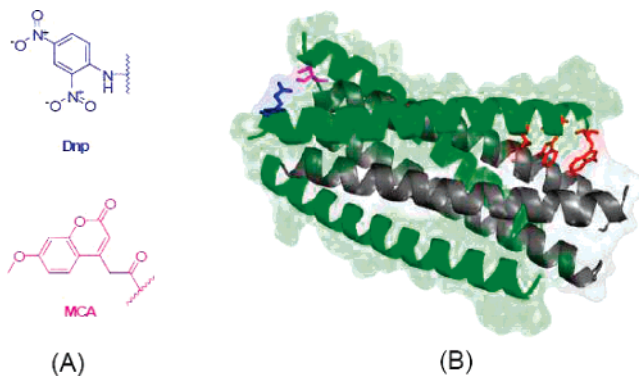
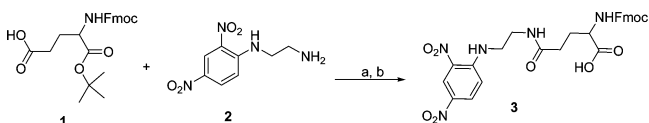


FIGURE 1. Structures of (A) the small-molecule FRET pair chosen for studies detailed in the text and (B) gp41 six-helix bundle core formed by N36 and C34. Residue S546 of one N-helix is highlighted in purple; residue E659 on one C-helix is highlighted in blue; key residues on C34 that are critical for binding to N36, Trp-628, Trp-631, and Ile-635 are highlighted in red.

SCHEME 1. Synthesis of Dnp Labeled Glutamic Acid 3^a



^a Reagents and conditions: (a) DIC, HOBt, DMF, 96%; (b) TFA, DCM, 87%.

especially prominent contacts with one of three symmetry-related, hydrophobic cavities on the surface of the coiled coil. Three amino acid residues of C34, Trp-628, Trp-631, and Ile-635 project into each of the cavities (Figure 1B), and they are critical for C34 binding to N36, forming the six-helix bundle complex. The study of Chan et al. provides strong evidence that these symmetrical coiled-coil cavities are good drug targets.

We have selected the N-terminus of residue S546 in the N36 peptide for the placement of the FRET donor MCA and the side chain carboxylic acid of E659 in the C34 peptide for the corresponding FRET quencher Dnp (Figure 1B). These locations were considered promising as they are solvent-exposed and therefore are unlikely to disturb the six-helix bundle assembly. In addition, their location is distal from the prominent binding pocket as revealed in previous studies.^{17,18}

Dnp labeled glutamic acid was synthesized following Scheme 1 and this modified amino acid was directly incorporated into the peptide synthesis. The Dnp labeled C34 peptide (C34Dnp) was prepared by automated, stepwise solid-phase peptide synthesis (SPPS) on a 1.0 mmol scale, using a DIC/HOBt protocol for Fmoc chemistry custom-written for a CSBio 136 automated peptide synthesizer (Scheme 2A). The MCA labeled N36 (N36MCA) was prepared in a similar fashion (Scheme 2B), with the N-terminus capped by MCA prior to the cleavage step. Both labeled peptides were purified by preparative RP-HPLC. The eluting fractions that were considered pure were pooled and analyzed by analytical RP-HPLC (Figure 2). MS analysis was conducted to confirm the identity of the full-length product (Figure 3). Unlabeled C34 and N36 were also prepared for future comparison.

2. Biophysical Analysis of FRET Labeled Peptides. As reported previously, C34 and N36 exist as mainly random coils

(11) Kilby, J. M.; Hopkins, S.; Venetta, T. M.; DiMassimo, B.; Cloud, G. A.; Lee, J. Y.; Alldredge, L.; Hunter, E.; Lambert, D.; Bolognesi, D.; Mathews, T.; Johnson, M. R.; Nowak, M. A.; Shaw, G. M.; Saag, M. S. *Nat. Med.* **1998**, *4*, 1302–1307.

(12) Kilgore, N. R.; Salzwedel, K.; Reddick, M.; Allaway, G. P.; Wild, C. T. *J. Virol.* **2003**, *77*, 7669–7672.

(13) Shu, W.; Liu, J.; Ji, H.; Radigen, L.; Jiang, S. B.; Lu, M. *Biochemistry* **2000**, *39*, 1634–1642.

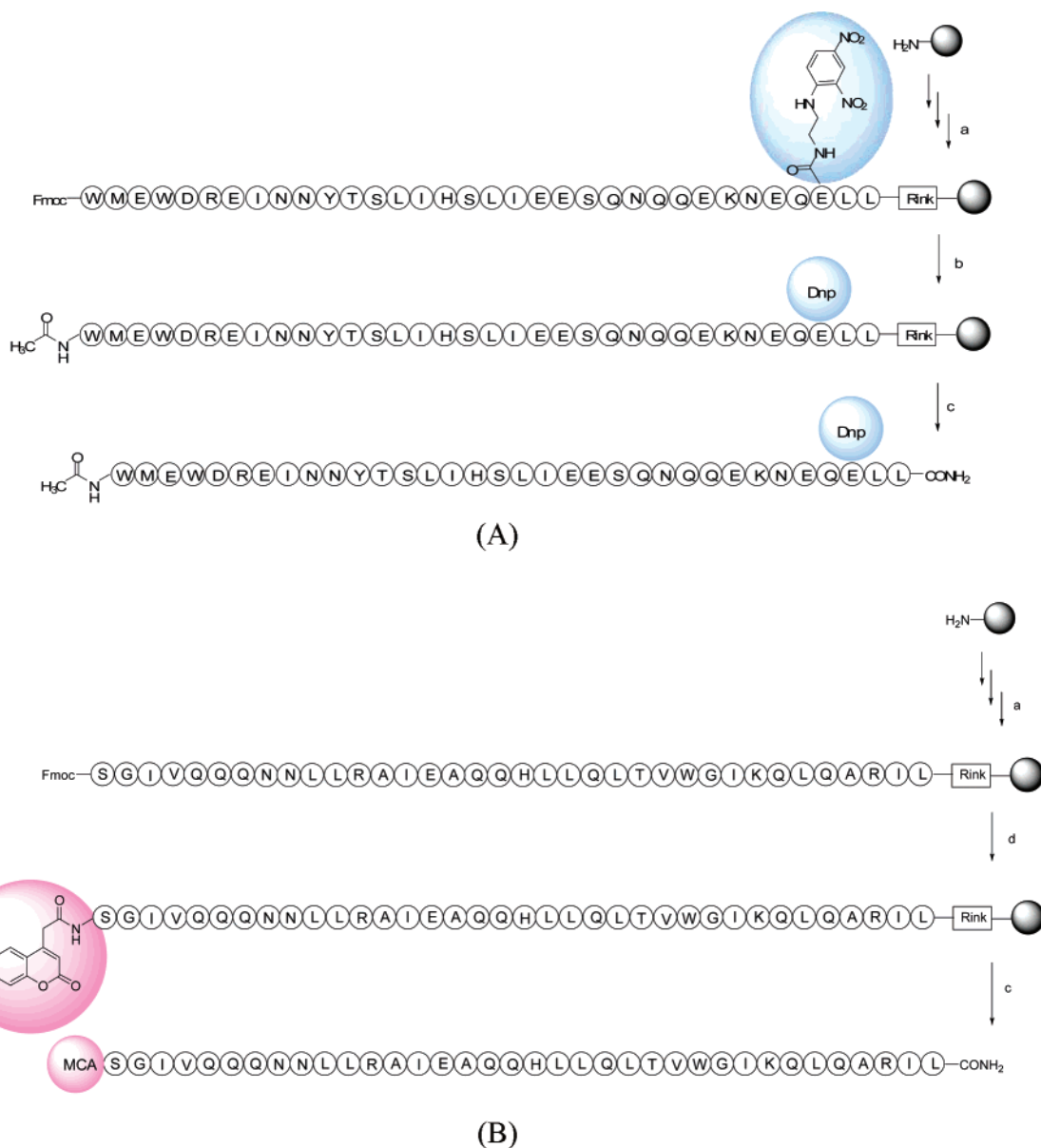
(14) Jiang, S. B.; Lin, K.; Zhang, L.; Debnath, A. K. *J. Virol. Methods* **1999**, *80*, 85–96.

(15) Zhao, Q.; Lu, H.; Schols, D.; De Clercq, E.; Jiang, S. B. *AIDS Res. Hum. Retroviruses* **2003**, *19*, 947–955.

(16) Liu, S. W.; Boyer-Chatenet, L.; Lu, H.; Jiang, S. B. *J. Biomol. Screening* **2003**, *8*, 685–693.

(17) Ji, H.; Shu, W.; Burling, F. T.; Jiang, S. B.; Lu, M. *J. Virol.* **1999**, *73*, 8578–8586.

(18) Chan, D. C.; Chutkowski, C. T.; Kim, P. S. *Proc. Natl. Acad. Sci. U.S.A.* **1998**, *95*, 15613–15617.

SCHEME 2. SPPS of C34Dnp (A) and N36MCA (B)^a

^a Reagents and conditions: (a) stepwise Fmoc SPPS with DIC/HOBt chemistry; (b) (i) 20% piperidine/DMF; (ii) acetic anhydride, DIEA (4 equiv); (c) TFA:water:TIPS (95:2.5:2.5); (d) (i) 20% piperidine/DMF; (ii) 7-methoxycoumarinyl-4-acetic acid, DIC, HOBt (4 equiv each), DMF.

in solution when separated; only upon complexation with each other will the two peptides fold into helices, coexisting in the form of a six-helix bundle.^{13,18} We conducted a circular dichroism (CD) spectral analysis of the C34-Dnp N36MCA hexameric bundle to see if comparable secondary structure was formed. The purified, lyophilized C34Dnp and N36MCA were reconstituted in phosphate-buffered saline (PBS), pH 7.4 at 100 μ M, and the two peptides were then mixed (1:1) to obtain a 20 μ M solution containing 5% ethanol as cosolvent. After 12 h of equilibration, this solution was examined by far-UV CD analysis and compared with a solution of unlabeled C34 and N36 (1:1 mixture, 25 μ M). After overnight incubation, no gross change in the helicity of the C34Dnp/N36MCA was observed (Figure 4) both with regard to intensity and the wavelength of global and local minima (208 and 222 nm, respectively), consistent with the stability observed with native N36/C34 hexameric complex. CD studies of the peptide complex formed by C34Dnp

and N36MCA revealed that these two peptides indeed form a complex, closely mimicking C34/N36 assembly, albeit with slightly reduced helical content and thermostability (Table 1).

CD spectra of individual peptide C34Dnp and N36MCA were also examined. The CD spectrum revealed that peptide C34Dnp in solution remained mostly as a random coil, a well-known characteristic shared by the native C34 peptide.¹⁹ On the other hand, the CD spectrum of N36MCA is consistent with a partial helical conformation, closely mimicking native N36 peptide under the same conditions.^{19,20} Our FRET-labeled peptides displayed comparable secondary structure as judged by CD studies; hence, only upon complexation do the two FRET-labeled peptides exhibit predominantly helical conformations. Furthermore, X-ray studies of unlabeled N36/C34 hexameric

(19) Kligler, Y.; Shai, Y. *J. Mol. Biol.* **2000**, *295*, 163–168.

(20) Kligler, Y.; Aharoni, A.; Rapaport, D.; Jones, P.; Blumenthal, R.; Shai, Y. *J. Biol. Chem.* **1997**, *272*, 13496–13505.

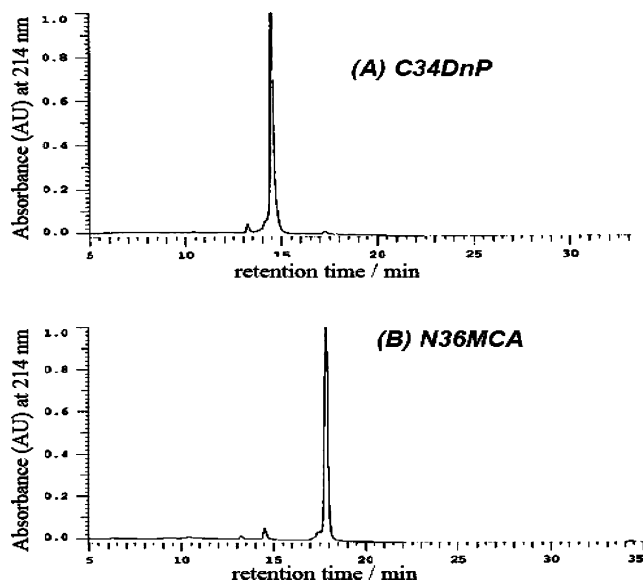


FIGURE 2. Analytical RP-HPLC for the purified (A) C34Dnp and (B) N36MCA.

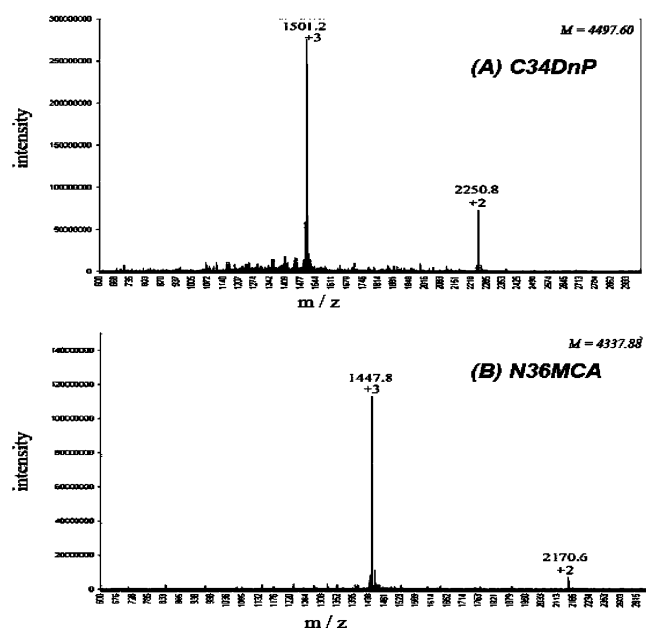


FIGURE 3. Raw ESI-MS data for the purified (A) C34Dnp and (B) N36MCA.

TABLE 1. CD Measurements of N36MCA/C34Dnp Complex and N36/C34 Complex

peptide complex	$[\theta]_{222}$ ($10^3 \text{ deg cm}^2 \text{ dmol}^{-1}$)	T_m ($^{\circ}\text{C}$)
N36/C34	-32.4	59
N36MCA/C34Dnp	-29.7	55

bundle have revealed that the 6-helix bundle conformation is universal in solution.²¹ On the basis of these observations, we believe that the perturbation of our FRET system is minimal upon peptide modification and our FRET-labeled N36 and C34 should form a hexameric bundle, closely mimicking the native N36/C34 complexation.

(21) Weissenhorn, W.; Dessen, A.; Harrison, S. C.; Skehel, J. J.; Wiley, D. C. *Nature* **1997**, *387*, 426–430.

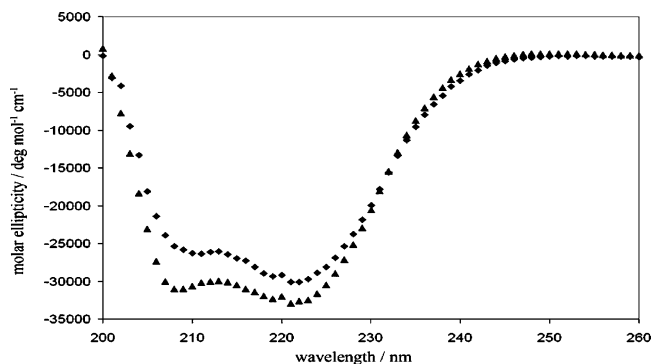


FIGURE 4. CD studies of the synthetic C34Dnp/N36MCA assembly and the C34/N36 six-helix bundle: (▲) CD scan of C34/N36 complex and (■) CD scan of C34Dnp/N36MCA complex.

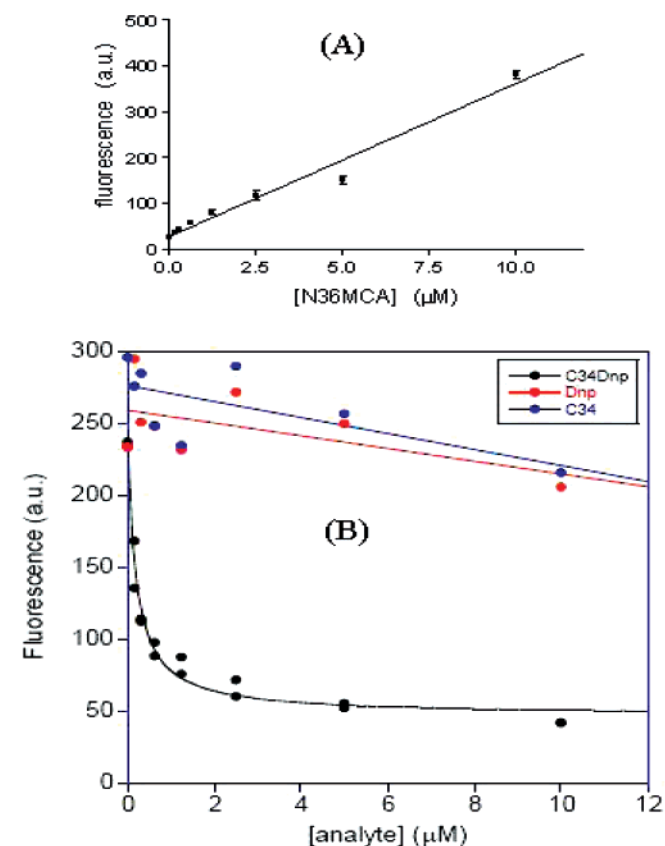


FIGURE 5. Characterization of the FRET system using fluorescence assays: (A) standard curve of donor peptide N36MCA and (B) titration of 5 μM N36MCA using quencher peptide C36Dnp.

3. Characterization of the FRET System with Use of Fluorescence-Based Assays. The fluorescence emission ($E_{\text{ex}} = 325 \text{ nm}$; $E_{\text{em}} = 445 \text{ nm}$) of donor peptide (N36MCA) was measured (Figure 5A) over a range of peptide concentrations. The observed fluorescence increased as a linear function with respect to the donor peptide concentration indicating that self-quenching of the donor peptide did not occur. On the other hand, when a 5 μM solution of donor peptide N36MCA was titrated with the quencher peptide C34Dnp a dose-dependent quenching profile (Figure 5B) resulted consistent with the generation of a FRET pair between the donor and quencher peptides. Interestingly, the observed half-maximal quenching concentration was $0.2 \pm 0.03 \mu\text{M}$, rather than the anticipated 2.5 μM based on

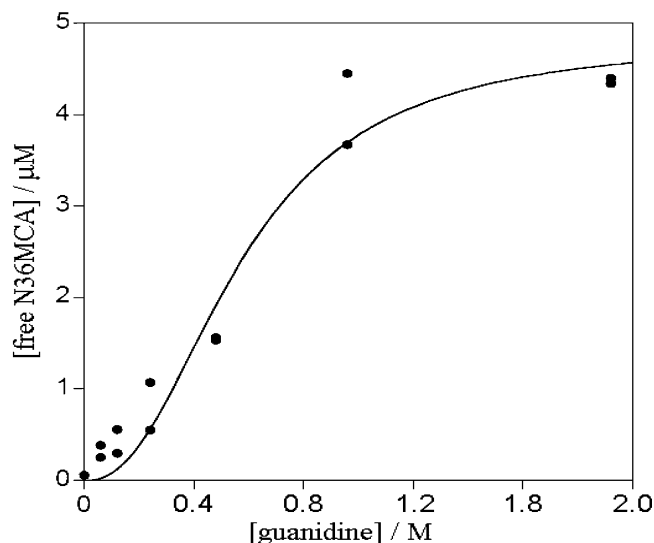


FIGURE 6. Guanidine denaturation curve for N36MCA/C34Dnp complex.

the 3-for-3 bundling of the peptides and the apparent tight binding reported previously.

In contrast to the quenching observed upon C34Dnp addition, dinitrophenylaniline and the native peptide C34 when titrated displayed marginal nonspecific quenching effects at the same concentrations tested (Figure 5B).

4. Guanidine Denaturation. To get a better grasp on how difficult it would be to disrupt the hexameric bundle, we investigated its stability toward the chaotropic agent guanidine hydrochloride. Donor peptide N36MCA ($5 \mu\text{M}$) and quencher peptide C34Dnp ($5 \mu\text{M}$) were mixed in PBS buffer and left at room temperature for 30 min to allow sufficient time for bundle formation. To this mixture was added guanidine (6 M solution) gradually. The fluorescence emission was noted after each guanidine addition. From these observations, guanidine induced the dissociation of the hexameric N36MCA-C34Dnp bundle, leading to the regeneration of the fluorescence by the freed N36MCA (Figure 6). The folded form of N36MCA is in essence spectrally silent as it exists in a FRET pair; therefore, we corrected for the change of fluorescence efficiency with N36MCA peptide in the absence of binding partner at varying guanidine concentrations.

$$[N36MCA]_{\text{free}} = 5 \mu\text{M} \frac{\text{fluorescence}_{\text{observed}}}{\text{fluorescence}_{\mu\text{MN36MCA}}} \quad (1)$$

This study showed that chaotropic reagent guanidine is able to disrupt the co-association between the FRET peptides, releasing free N36MCA as monitored by an increase of fluorescence.

5. Displacement of the $2 \mu\text{M}$ N36MCA/C34Dnp Hexameric Bundle with Use of Unlabeled Peptide C34. Although we know from the CD spectrum and the FRET induced loss of fluorescence that the peptides form a tight hexameric bundle, it is possible that a small amount of the peptide exists in the dissociated state. If so, it should be possible to exchange/displace the C34Dnp with C34 resulting in a return of the N36MCA fluorescence. To investigate this possibility and to determine the rate of potential exchange, a solution of $2 \mu\text{M}$ N36MCA/C34Dnp hexameric bundle was prepared by mixing N36MCA ($6 \mu\text{M}$) and C34Dnp ($6 \mu\text{M}$) in PBS at room temperature. The solution was allowed to stand at room temperature for 30 min. Following the addition of unlabeled peptide C34 over a range of concentrations, the fluorescence was measured continuously over 2 h. As shown in Figure 7A peptide C34 displaced C34Dnp leading to the regeneration of fluorescence of N36MCA. This displacement assay demonstrated an exponential profile to equilibrium and, at equilibrium, gives saturation.

The half time to full C34 displacement ($T_{1/2}$) is 17 ± 5 min based on eq 2. The change in fluorescence for the system should

$$F = F_{\text{MAX}}(1 - e^{-kt}) + F_0 \quad (2)$$

be proportional to the change in the concentration of C34Dnp bound in the hexameric bundles. As the C34Dnp is replaced by C34 the quenching of N36MCA diminishes and fluorescence increases. A C34 binding site must open first and then C34 and C34DNP compete for its occupancy. Increasing the concentration of C34 increases the probability that the site will be occupied by C34 rather than C34DNP. Upon establishment of equilibrium (which itself will reflect the ratio of the binding constants of C34 and C34DNP for the N36MCA peptide bundle), a stable fluorescence is observed and is reflective of the ratio of C34 to C34DNP bound. The observed saturation end points were fit to eq 3, vide infra.

In an effort to understand the C34 disruption of the FRET-labeled hexameric bundle, we studied the C34 displacement in

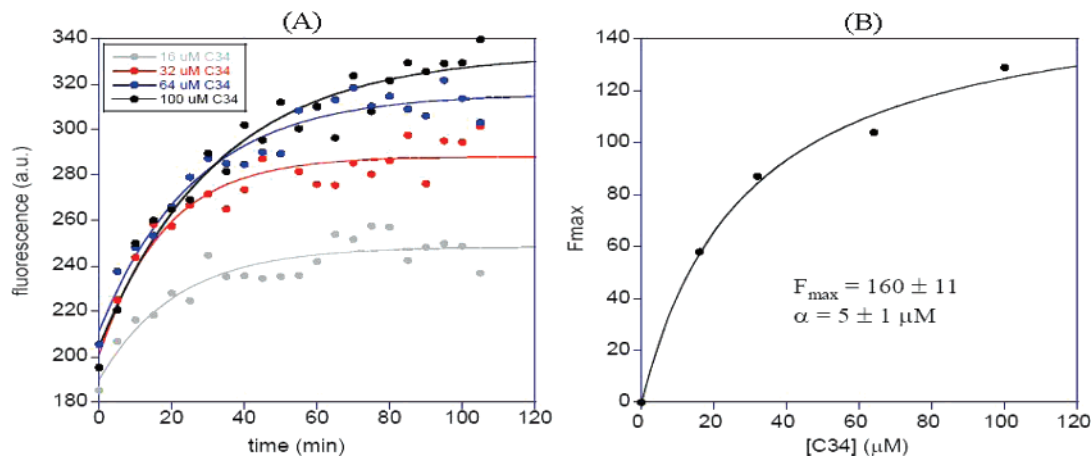


FIGURE 7. C34 displacement of $2 \mu\text{M}$ N36MCA/C34Dnp hexameric bundle: (A) time-dependent C34 displacement profile and (B) dose-dependent C34 displacement of hexameric peptide bundle.

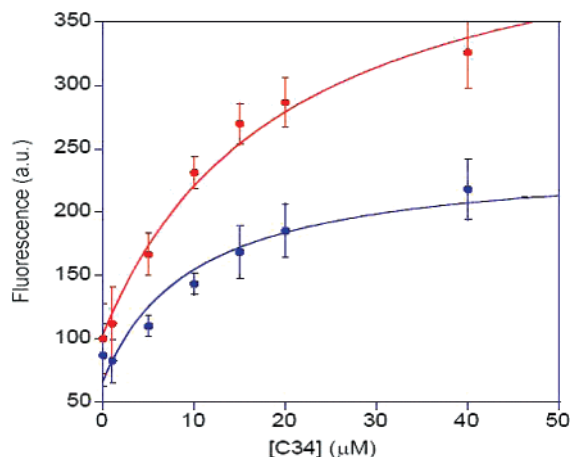


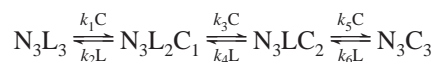
FIGURE 8. Single cuvette studies of C34 displacement of N36MCA/C34Dnp hexameric bundle: (blue) 1 μM N36MCA mixed with 1 μM C34Dnp and (red) 2 μM N36MCA mixed with 2 μM C34Dnp.

single cuvette assays, where the increased reaction volume of 3 mL was expected to give greater accuracy. The results of single cuvette assays are in accordance with previous displacement experiments performed in the microtiter plate (Figure 8).

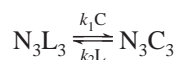
The hexameric bundle can be thought of as a tightly bound complex of (3) N36MCA and (3) C34DNP. Given the observation of increased fluorescence over time with increasing amounts of unlabeled C34 we know that exchange is possible although it is slow (with a half time of 17 min). The fluorescence profiles shown in Figure 7B as well as the one shown in our single cuvette assays (Figure 8) display saturating behavior. Since the dissociation constant for the hexamer is apparently much less than 1 μM and in fact should approach nanomolar as previously reported from Luciferase and syncytia formation assay systems,¹⁸ the concentration of C34 causing fluorescence half saturation is not a reflection of K_D but rather a function of dilution via mass action. Basically the profile should produce the fluorescence of free N36MCA multiplied by the mole fraction of C34.

The simplest model consistent with these observations is a displacement where each C34 peptide behaves identically and each C34Dnp also behaves identically, but C34 and C34Dnp may have differential binding for N36MCA.

The complete displacement scheme is shown below



where L = C34Dnp and C = C34. If $k_1 = k_3 = k_5$ and $k_2 = k_4 = k_6$ (binding of C34 or C34Dnp is independent of the other C34 species in the hexameric bundle) the displacement scheme reduces to (where L = C34Dnp and C = C34)



$$[\text{N}_3\text{C}_3] = \frac{[\text{C}]}{[\text{C}] + \frac{k_2}{k_1}[\text{L}]} N_{\text{Total}} (1 - e^{-k_{\text{obs}}t})$$

$$\text{where } k_{\text{obs}} = k_1[\text{C}] + k_2[\text{L}]$$

and at equilibrium

$$[\text{N}_3\text{C}_3] = \frac{[\text{C}]}{[\text{C}] + \frac{k_2}{k_1}[\text{L}]} N_{\text{Total}}$$

The equation consistent with this simplified model is shown below (see Supporting Information for full derivation):

$$f = \frac{F_{\text{MAX}}[\text{C34}]}{[\text{C34}] + \alpha[\text{C34DNP}]} + f_0 \quad (3)$$

The correcting parameter α consists of the differential in the binding constants for the C34 versus the C34DNP as well as the average quenching efficiency of one C34DNP (see the Supporting Information). Here, α was found equal to 10 ± 2 , while F_{MAX} is the intrinsic fluorescence of N36MCA when complexed with C34. Unlabeled peptide N36 also demonstrated a time-dependent displacement of the FRET-labeled hexameric bundle, albeit with lower proficiency and consistent with previous reports.^{22,23} The half time for full N36 displacement ($T_{1/2}$) is approximately 10 min.

$$[\text{C34Dnp}]/K_D^{\text{app}} = [\text{Inhibitor}]/K_i$$

Since C34 displacement is observed, it should be possible for small molecule or peptide inhibitors targeting gp41 to disrupt the FRET-labeled hexameric bundle. The potency of such an inhibitor will be reflected by the concentration required to disrupt the FRET system. In effect the N36MCA-C34Dnp FRET system is a competition assay where the observed fluorescence is proportional to the ratio of test compound over its K_D versus the concentration of C34Dnp over its K_D . While the absolute value of a test compound's K_D may be difficult to determine, an apparent K_D akin to an IC_{50} is possible. Compounds examined under identical conditions may be ranked in terms of their apparent K_D values. A more potent inhibitor will disrupt C34Dnp complexation with N36MCA at a lower concentration than a weaker compound. When screening chemical libraries using our FRET system, we believe that we can not only seek out potential inhibitors but also rank them in terms of potency prior to further testing via cell-based assays.

Conclusion

We have designed, synthesized, and validated a FRET-labeled N36/C34 hexameric system with an apparent dissociation constant of much less than 1 μM , but with the capability of slow exchange with its unlabeled monomeric subunits ($T_{1/2}$ of 17 min). As such, while tightly associated, the hexameric bundle may be disrupted. This system may also be destabilized by chaotropic agents such as guanidine hydrochloride. The assay can be run on a fluorescence microplate reader, which leads readily to automation. In total, we believe our FRET system will have utility in the discovery of small molecules capable of disrupting gp41 core assembly. Such molecules are potential therapeutic agents as HIV fusion inhibitors.

Experimental Section

tert-Butyl 2-(((9H-Fluoren-9-yl)methoxy)carbonylamino)-5-(2-(2,4-dinitrophenylamino)ethylamino)-5-oxopentanoate. To a solution of 4-(((9H-fluoren-9-yl)methoxy)carbonylamino)-5-tert-

(22) Liu, S. W.; Jiang, S. B. *Curr. Pharm. Des.* **2004**, *10*, 1827–1843.

(23) Liu, S. W.; Zhao, Q.; Jiang, S. B. *Peptides* **2003**, *24*, 1303–1313.

butoxy-5-oxopentanoic acid **1** (4.5 g, 10.6 mmol) in DMF (100 mL) were added DIC (0.5 M in DMSO, 70 mL, 35 mmol) and HOBt (1.7 g, 35 mmol). The mixture was stirred at room temperature for 30 min and then *N*¹-(2,4-dinitrophenyl)ethane-1,2-diamine (**2**) (2.0 g, 8.8 mmol) was added to the mixture. The reaction was left at room temperature for 10 h and concentrated in vacuo to remove DMF. The mixture was then diluted with 50% EtOAc/hexane (500 mL) and washed 3 times with water (500 mL). The organic layer was dried over Mg SO₄ and concentrated. The crude product was purified by flash column chromatography on silica gel (50% EtOAc/Hex) to give *tert*-butyl 2-(((9*H*-fluoren-9-yl)methoxy)carbonylamino)-5-(2-(2,4-dinitrophenylamino)ethylamino)-5-oxopentanoate (5.4 g, 8.5 mmol, 96% yield) as a yellow solid.

¹H NMR (500 MHz, CDCl₃) δ 9.15 (s, 1H), 8.81 (s, 1H), 8.31 (d, *J* = 9.45 Hz, 1H), 7.84 (d, *J* = 7.5 Hz, 2H), 7.67 (t, *J* = 7.72 Hz, 2H), 7.49 (t, *J* = 7.12 Hz, 2H), 7.40 (t, *J* = 7.45 Hz, 2H), 7.34 (d, *J* = 0.98 Hz, 1H), 7.09 (d, *J* = 7.48 Hz, 1H), 6.86 (s, 1H), 5.66 (d, *J* = 7.60, 1H), 4.50 (m, 2H), 4.28 (m, 2H), 3.69 (m, 4H), 2.42 (m, 2H), 1.99 (m, 1H), 1.76 (m, 1H), 1.54 (s, 9H). ¹³C NMR (125 MHz, CDCl₃) δ 173.1, 170.7, 156.7, 148.3, 143.7, 141.2, 141.2, 136.22, 130.6, 130.3, 127.7, 127.0, 125.0, 124.9, 124.1, 120.0, 113.9, 83.0, 77.2, 77.0, 76.7, 67.1, 60.3, 53.6, 47.0, 43.0, 38.3, 32.49, 29.6, 27.9, 21.0, 14.1. ESI-TOF calcd for C₃₂H₃₅N₅O₉ [M + H⁺] 634.2507, found 634.2500.

2-(((9*H*-fluoren-9-yl)methoxy)carbonylamino)-5-(2-(2,4-dinitrophenylamino)ethylamino)-5-oxopentanoic Acid (3**).** To a solution of *tert*-butyl 2-(((9*H*-fluoren-9-yl)methoxy)carbonylamino)-5-(2-(2,4-dinitrophenylamino)ethylamino)-5-oxopentanoate **3** (5.4 g, 8.5 mmol) in DCM (100 mL) was added TFA (100 mL). The reaction was left at room temperature for 5 h then concentrated in vacuo to remove TFA. The crude product was purified by flash column chromatography on silica gel (10% H₂O/ MeCN) to give 2-(((9*H*-fluoren-9-yl)methoxy)carbonylamino)-5-(2-(2,4-dinitrophenylamino)ethylamino)-5-oxopentanoic acid (**3**) (4.3 g, 7.4 mmol, 87% yield) as a yellow solid.

¹H NMR (400 MHz, MeOD) 8.97 (s, 1H), 8.81 (m, 1H), 8.22 (d, *J* = 9.60 Hz, 1H), 7.76 (t, *J* = 7.54 Hz, 2H), 7.65 (t, *J* = 8.10 Hz, 2H), 7.37 (t, *J* = 7.39 Hz, 2H), 7.30 (t, *J* = 7.43, 2H), 7.18 (d, *J* = 9.57, 1H), 4.35 (m, 2H), 4.18 (m, 2H), 3.57 (m, 4H), 2.32 (t, *J* = 6.80 Hz, 2H), 2.19 (m, 1H), 1.95 (m, 1H). ¹³C NMR (100 MHz, MeOD) 188.8, 175.7, 158.5, 149.7, 145.2, 142.4, 130.9, 128.7, 128.1, 127.2, 126.2, 126.2, 120.9, 115.6, 110.6, 67.9, 48.3, 43.9, 42.7, 39.1, 33.2, 28.7, 23.5. ESI-TOF calcd for C₂₈H₂₇N₅O₉ [M + H⁺] 578.1881, found 578.1873.

Synthesis of Peptide C34. Peptide C34 was prepared on a 1.0 mmol scale with use of custom-written DIC/HOBt protocols for Fmoc SPPS on an automated peptide synthesizer. Global deprotection and cleavage of the peptide-resin anchorage was accomplished by batchwise treatment with 95:2.5:2.5 TFA:water:triisopropylsilane (TIPS) for 2 h, followed by filtration and removal of TFA by rotary evaporation at room temperature. The peptide was then triturated from 10 volumes of Et₂O (prechilled at -20 °C) and isolated by centrifugation. After likewise washing the pellet three times further with Et₂O, the peptide was extracted into 50% MeCN/water and lyophilized over 2 days. The dried peptide was then redissolved in 50% AcOH and purified by RP-HPLC. Isolated yield after lyophilization is 130 mg (3.0%).

ESI-MS theoretical, MW = 4289.6; M²⁺ = 2145.8, M³⁺ = 1430.8; observed M²⁺ = 2146.5, M³⁺ = 1431.8.

Synthesis of Peptide C34Dnp. Peptide C34Dnp was prepared on a 1.0 mmol scale with use of custom-written DIC/HOBt protocols for Fmoc SPPS on an automated peptide synthesizer and is depicted in Scheme 2. Dnp labeled Glutamic acid **4** was incorporated into this stepwise synthetic process. Global deprotection and cleavage of the peptide-resin anchorage was accomplished by batchwise treatment with 95:2.5:2.5 TFA:water:triisopropylsilane (TIPS) for 2 h, followed by filtration and removal of TFA by rotary evaporation at room temperature. The peptide was then triturated

from 10 volumes of Et₂O (prechilled at -20 °C) and isolated by centrifugation. After likewise washing the pellet three times further with Et₂O, the peptide was extracted into 50% MeCN/water and lyophilized over 2 days. The dried peptide was then redissolved in 50% AcOH and purified by RP-HPLC. Isolated yield after lyophilization is 115 mg (2.5%).

ESI-MS theoretical, MW = 4497.6; M²⁺ = 2249.8, M³⁺ = 1500.2; observed M²⁺ = 2250.8, M³⁺ = 1501.2.

Synthesis of Peptides N36 and N36MCA. Peptide N36 was prepared on a 1.0 mmol scale with use of custom-written DIC/HOBt protocols for Fmoc SPPS on an automated peptide synthesizer. After removal of the N-terminal Fmoc group, the resin was divided equally into two portions. To one portion acetic anhydride (5 mmol) and DIEA (5 mmol) were added to produce the terminal amide of N36 peptide. To the other portion 7-methoxycoumarinyl-4-acetic acid was coupled according to standard DIC/HOBt protocols to give N36MCA peptide. Global deprotection and cleavage of the peptide-resin anchorage was accomplished by batchwise treatment with 95:2.5:2.5 TFA:water:triisopropylsilane (TIPS) for 2 h, followed by filtration and removal of TFA by rotary evaporation at room temperature. Both peptides were then triturated from 10 volumes of Et₂O (prechilled at -20 °C) and isolated by centrifugation. After likewise washing the pellet three times further with Et₂O, the peptides were extracted into 50% MeCN/water and lyophilized over 2 days. The dried peptides were then redissolved in 50% AcOH and purified by RP-HPLC. Isolated yield of N36 after lyophilization was 79 mg (3.9%); isolated yield of N36MCA was 76 mg (3.5%).

N36 ESI-MS theory, MW = 4163.9; M²⁺ = 2083.0, M³⁺ = 1389.0; observed, M²⁺ = 2083.5, M³⁺ = 1389.5.

N36MCA ESI-MS theory, MW = 4337.9; M²⁺ = 2170.0, M³⁺ = 1446.9; observed, M²⁺ = 2170.6, M³⁺ = 1447.8.

CD Measurements. Far-UV circular dichroism spectra were obtained with a 1 cm path length fused silica cell at 4 °C. Purified peptides, C34, C34Dnp, N36, and N36MCA, were reconstituted at 100 μM. Both of the peptides C34Dnp and N36MCA were diluted 5-fold into a solution in phosphate-buffered saline, pH 7.4, containing 5 vol % EtOH. Data were corrected for blank absorbance of each compound, and are reported as the average of three scans. The CD spectrum of a C34/N36 complex was measured in the same manner. Thermal stability was determined by monitoring the change in [θ]₂₂₂ as a function of temperature. Thermal melts were performed in 2 deg increments with an equilibration time of 120 s at the desired temperature and an integration time of 30 s. The apparent *T*_m was estimated from the thermal dependence of the CD signal at 222 nm.

Characterization of the FRET System by Using a Series of Fluorescence-Based Assays. All fluorescence measurements were performed with excitation at 325 nm. The fluorescence emission (*E*_{em} = 445 nm) of donor peptide was measured at a range of peptide concentrations in PBS buffer (10 mM, 100 mM NaCl, pH 7.4), containing 5 vol % EtOH, at room temperature in a BSA-precoated 96-well EIA/RIA plate (1/2 area, flat bottom). In a typical titration assay, quencher was added to the N36MCA solution (5 μM) in PBS in a sequential manner. The fluorescence emission was then measured at 445 nm and data were corrected for the actual volume of the peptide solution.

Displacement of the 2 μM N36MCA/C34Dnp Hexameric Bundle by Using Unlabeled Peptide C34 or N36. A solution of 2 μM N36MCA/C34Dnp hexameric bundle was prepared by mixing N36MCA (6 μM) and C34Dnp (6 μM) in PBS, containing 5 vol % EtOH, at room temperature in a BSA-precoated 96-well EIA/RIA plate (1/2 area, flat bottom). The solution was allowed to stand at room temperature for 30 min. Following the addition of unlabeled peptide C34 (final concentration 16 μM) and a final volume of 200 μL, the fluorescence emission at 445 nm was measured every 10 min over a period of 2 h. The assay was repeated at three other C34 concentrations, 32, 64, and 100 μM. The same displacement assays were performed with N36.

Single Cuvette Studies of Displacement of the N36MCA/C34Dnp Hexameric Bundle by Using Unlabeled Peptide C34. A solution of N36MCA/C34Dnp hexameric bundle was prepared by mixing N36MCA (1 μ M) and C34Dnp (1 μ M) in PBS, containing 5 vol % EtOH, at room temperature in a quartz cuvette. The solution was allowed to stand at room temperature for 30 min. Following the addition of unlabeled peptide C34 (final concentration 1 μ M) and final volume of 3 mL, the fluorescence emission at 445 nm was measured after 2 h. The assay was repeated at five other C34 concentrations, 5, 10, 15, 20, and 40 μ M.

Acknowledgment. We would like to thank Dr. Shibo Jiang, Dr. Laura A. McAllister, Dr. Florence Brunel, Jason Chen, Dr.

Youngsoo Kim, and Dr. Jason Moss for fruitful discussions and suggestions. This work was supported by Skaggs Institute for Chemical Biology and Scripps Neuro-Aids Preclinical Studies (SNAPS) (2P30 MH062261).

Supporting Information Available: The full-displacement kinetic model and NMR spectra of compounds *tert*-butyl 2-(((9*H*-fluoren-9-yl)methoxy)carbonylamino)-5-(2-(2,4-dinitrophenylamino)ethylamino)-5-oxopentanoate and **3**. This material is available free of charge via the Internet at <http://pubs.acs.org>.

JO070836L